



This is a repository copy of *How many phosphoric acid units are required to ensure uniform occlusion of sterically-stabilized nanoparticles within calcite?*.

White Rose Research Online URL for this paper:
<https://eprints.whiterose.ac.uk/145902/>

Version: Supplemental Material

Article:

Douverne, M., Ning, Y., Tatani, A. et al. (2 more authors) (2019) How many phosphoric acid units are required to ensure uniform occlusion of sterically-stabilized nanoparticles within calcite? *Angewandte Chemie International Edition*, 58 (26). pp. 8692-8697. ISSN 1433-7851

<https://doi.org/10.1002/anie.201901307>

This is the peer reviewed version of the following article: Douverne, M. , Ning, Y. , Tatani, A. , Meldrum, F. . and Armes, S. . (2019), How Many Phosphoric Acid Units Are Required to Ensure Uniform Occlusion of Sterically-Stabilized Nanoparticles within Calcite?. *Angew. Chem. Int. Ed.*, which has been published in final form at <https://doi.org/10.1002/anie.201901307>. This article may be used for non-commercial purposes in accordance with Wiley Terms and Conditions for Use of Self-Archived Versions.

Reuse

Items deposited in White Rose Research Online are protected by copyright, with all rights reserved unless indicated otherwise. They may be downloaded and/or printed for private study, or other acts as permitted by national copyright laws. The publisher or other rights holders may allow further reproduction and re-use of the full text version. This is indicated by the licence information on the White Rose Research Online record for the item.

Takedown

If you consider content in White Rose Research Online to be in breach of UK law, please notify us by emailing eprints@whiterose.ac.uk including the URL of the record and the reason for the withdrawal request.



eprints@whiterose.ac.uk
<https://eprints.whiterose.ac.uk/>

How Many Phosphoric Acid Units Are Required to Ensure Uniform Occlusion of Sterically-Stabilized Nanoparticles within Calcite?

Marcel Douverne,^[a,b] Yin Ning,^[*,a] Aikaterini Tatani,^[a] Fiona C. Meldrum^[c] and Steven P. Armes^[*,a]

^a Department of Chemistry, University of Sheffield, Brook Hill, Sheffield, South Yorkshire S3 7HF, U.K.

^b Faculty of Chemistry, Pharmaceutical Sciences and Geosciences, Johannes Gutenberg-University Mainz, Duesbergweg 10-14, 55128 Mainz, Germany.

^c School of Chemistry, University of Leeds, Woodhouse Lane, Leeds, LS2 9JT, U.K.

E-mail: Y.Ning@sheffield.ac.uk; s.p.arnes@sheffield.ac.uk

Contents

1. Experimental Section	3
1.1. Materials	3
1.2. Synthesis of poly(glycerol monomethacrylate) ₅₁ [G ₅₁] macro-CTA.....	3
1.3. Synthesis of poly(glycerol monomethacrylate) ₅₁ -poly(benzyl methacrylate) ₃₀₀ [G ₅₁ -B ₃₀₀] diblock copolymer nanoparticles via RAFT aqueous emulsion polymerization	3
1.4. Synthesis of poly(2-(phosphonooxy)ethyl methacrylate) _x [P _x] macro-CTA.....	3
1.5. Synthesis of poly(2-(phosphonooxy)ethyl methacrylate) ₅₁ -poly(benzyl methacrylate) ₃₀₀ (P _x -B ₃₀₀) diblock copolymer nanoparticles	4
1.6. Synthesis of poly(2-(phosphonooxy)ethyl methacrylate) _x - <i>stat</i> -poly(glycerol monomethacrylate) _y macro-CTAs [(P _x - <i>stat</i> -G _y) macro-CTA]	4
1.7. Synthesis of poly(2-(phosphonooxy)ethyl methacrylate) _x - <i>stat</i> -poly(glycerol monomethacrylate) _y -poly(benzyl methacrylate) ₃₀₀ [(P _x - <i>stat</i> -G _y)-B ₃₀₀] nanoparticles.....	4
1.8. Precipitation of calcium carbonate crystals in the presence of nanoparticles	5
2. Characterization	5
2.1. ¹ H NMR spectroscopy	5
2.2. Gel permeation chromatography (GPC)	5
2.3. Dynamic light scattering (DLS)	5
2.4. Transmission electron microscopy (TEM).....	6
2.5. Scanning electron microscopy (SEM)	6
2.6. Other measurements.....	6
3. Supplementary Tables.....	7
Table S1.	7
Table S2.	7
4. Calculation of the average inter-particle distance (<i>d</i>)	8
5. Supplementary Figures	10
Figure S1.....	10
Figure S2.....	11
Figure S3.....	12
Figure S4.....	13
Figure S5.....	14
Figure S6.....	15
Figure S7.....	16
Figure S8.....	17
Figure S9.....	18
Figure S10.....	19
5. References.....	19

1. Experimental Section

1.1. Materials

Glycerol monomethacrylate (G; 99.8%) was supplied by GEO Specialty Chemicals (Hythe, UK) and 2-(phosphonoxy)ethyl methacrylate (P, containing ~10% dimethacrylate) was kindly donated by Solvay (France). Both monomers were used without further purification. 2,2'-Azobis(2-methylpropionitrile) (AIBN), 4,4'-azobis(4-cyanovaleric acid) (ACVA; 99%), 2-cyanoprop-2-yl dithiobenzoate (CPDB), benzyl methacrylate (BzMA), ammonium carbonate and calcium chloride hexahydrate were all purchased from Sigma-Aldrich (UK) and used as received. Deionized water was obtained from an in-house Elgastat Option 3A water purification unit. All solvents were obtained from Sigma-Aldrich (UK).

1.2. Synthesis of poly(glycerol monomethacrylate)₅₁ [G₅₁] macro-CTA

The synthesis of poly(glycerol monomethacrylate)₅₁ [G₅₁] macro-CTA was conducted as follows. CPDB RAFT agent (0.46 g, 2 mmol, ~80% purity), AIBN initiator (0.064 g, 0.4 mmol, CTA/ACVA molar ratio = 5.0) and anhydrous ethanol (30 g, 0.652 mol) were added to a round-bottomed flask containing a magnetic stirrer bar. When the CPDB and AIBN were fully dissolved, G monomer (20 g, 0.125 mol) was added to afford a target degree of polymerization (DP) of 60. This pink ethanolic solution was sparged with N₂ for 30 min, before the flask was placed in an oil bath set at 70 °C. The polymerization was quenched after 2 h by cooling the flask in an ice bath followed by exposure of its contents to air. The crude polymer was purified by precipitation into a ten-fold excess of dichloromethane (twice). The second precipitate was redissolved in water and the final pink polymer was obtained as a dry powder by lyophilisation overnight. ¹H NMR analysis indicated a mean DP of 51 for this G macro-CTA (the integrated signals from 0.5 ppm to 2.4 ppm assigned to the five backbone protons on the poly(glycerol monomethacrylate) units were compared to that of the aromatic signals of the five protons on the RAFT CTA end-group). DMF GPC analysis (data expressed relative to poly(methyl methacrylate) calibration standards) indicated *M_n* and *M_w/M_n* values of 12.9 kg mol⁻¹ and 1.18, respectively (see **Figure S2a**).

1.3. Synthesis of poly(glycerol monomethacrylate)₅₁-poly(benzyl methacrylate)₃₀₀ [G₅₁-B₃₀₀] diblock copolymer nanoparticles via RAFT aqueous emulsion polymerization

The synthesis of poly(glycerol monomethacrylate)₅₁-poly(benzyl methacrylate)₃₀₀ [G₅₁-B₃₀₀] diblock copolymer nanoparticles via RAFT aqueous emulsion polymerization was conducted as follows. G₅₁ macro-CTA (60 mg, 7.15 μmol) and ACVA initiator (0.40 mg, 1.43 μmol, macro-CTA/ACVA molar ratio = 5.0) were weighed into a 14 mL vial equipped with a magnetic stir bar and a rubber septum. Deionized water (2.5 g) was added and the resulting solution was stirred until all components were completely dissolved. Benzyl methacrylate (378 mg, 2.15 mmol) was added and the emulsion was degassed via N₂ sparge for 30 min. The vial was then transferred to a preheated oil bath set at 70 °C and the polymerization was conducted for 5 h. The reaction was quenched by exposing the resulting pink aqueous dispersion to air while cooling to ambient temperature. More than 99% monomer conversion was achieved, as determined by ¹H NMR spectroscopy.

1.4. Synthesis of poly(2-(phosphonoxy)ethyl methacrylate)_x [P_x] macro-CTA

The synthesis of poly(2-(phosphonoxy)ethyl methacrylate)_x [P_x] macro-CTA was conducted as follows. CPDB RAFT agent (234 mg, 1.1 mmol) and AIBN initiator (35 mg, 0.21 mmol, CPDB/AIBN molar ratio = 5) were added to a 250 mL round-bottomed flask equipped with a magnetic stir bar. These reagents were dissolved in methanol (118 g), 2-(phosphonoxy)ethyl methacrylate (6 g, 29 mmol) was then added and the stirred solution was degassed with N₂ for 30 min in an ice bath. The flask was transferred to an oil bath preheated to 70 °C and the polymerization was run for 6 h before quenching by cooling the flask using an ice bath, followed by exposure of its contents to air. The resulting polymer was purified by precipitation into a ten-fold excess of diethyl

ether (three times). The resulting moist precipitate was redissolved in water and the final polymer was obtained as a dry pink powder by lyophilization. A mean DP of 51 was calculated for this macro-CTA using ^1H NMR spectroscopy by comparing the integrated signal intensity assigned to the aromatic protons at 7.2-7.4 ppm with that due to the methacrylic backbone at 0.4-2.5 ppm. Aqueous GPC analysis (against a series of poly(ethylene oxide) calibration standards) indicated M_n and M_w/M_n values of 9.0 kg mol^{-1} and 1.34, respectively (see **Figure S2b**).

1.5. Synthesis of poly(2-(phosphonooxy)ethyl methacrylate)₅₁-poly(benzyl methacrylate)₃₀₀ (**P_x-B₃₀₀**) diblock copolymer nanoparticles

The synthesis of the poly(2-(phosphonooxy)ethyl methacrylate)₅₁-poly(benzyl methacrylate)₃₀₀ (**P_x-B₃₀₀**) diblock copolymer nanoparticles was conducted as follows. **P₅₁** macro-CTA (155 mg, 15.2 μmol), ACVA (0.85 mg, 3.04 μmol , macro-CTA/ACVA molar ratio = 5.0) were added to a 14 mL vial equipped with a magnetic stir bar. Methanol (3.2 g) was added to dissolve these two reagents and then benzyl methacrylate monomer (749 mg, 4.25 mmol) was added. The vial was sealed with a rubber septum and degassed with N_2 for 30 min, before being transferred to an oil bath preheated at 70 °C. The polymerization was quenched after 24 h by exposing the methanolic dispersion to air while cooling to ambient temperature. ^1H NMR studies indicated more than 99 % monomer conversion. The resulting diblock copolymer nanoparticles were centrifuged (11,000 rpm for 30 min) after being diluted to 1.0 wt% using deionized water. The aqueous supernatant was carefully decanted and the sedimented nanoparticles were redispersed in water. This centrifugation-redispersion cycle was repeated five times.

1.6. Synthesis of poly(2-(phosphonooxy)ethyl methacrylate)_x-stat-poly(glycerol monomethacrylate)_y macro-CTAs [(**P_x-stat-G_y**) macro-CTA]

The synthesis of the poly(2-(phosphonooxy)ethyl methacrylate)₃₂-stat-poly(glycerol monomethacrylate)₁₃ macro-CTA was conducted as follows. CPDB RAFT agent (211 mg, 0.95 mmol) and AIBN initiator (31 mg, 0.19 mmol, CPDB/AIBN molar ratio = 5.0) were added to a 250 mL round-bottomed flask equipped with a magnetic stir bar and a rubber septum. These reagents were dissolved in methanol (105 g) and then 2-(phosphonooxy)ethyl methacrylate (3.00 g, 14.3 mmol) and glycerol monomethacrylate (2.29 g, 14.3 mmol) were added. The flask was then placed in an ice bath and degassed with N_2 for 30 min before being transferred to an oil bath preheated to 70 °C. After 6 h, the copolymerization was quenched by exposing the contents of the flask to air, followed by cooling to ambient temperature. The reaction mixture was concentrated to 50 mL using a rotary evaporator and the polymer was precipitated into excess diethyl ether (600 mL). This purification protocol was repeated three times. The precipitate was redissolved in water and the final polymer was obtained as a dry pink powder by lyophilization. ^1H NMR studies indicated that the overall mean DP of this statistical copolymer was 55, of which 33 units with 2-(phosphonooxy)ethyl methacrylate units and 13 units were glycerol monomethacrylate. Other (**P_x-stat-G_y**) macro-CTAs were synthesized using a similar protocol by varying the P/G comonomer molar ratio, as summarized in **Table S2** (see below).

1.7. Synthesis of poly(2-(phosphonooxy)ethyl methacrylate)_x-stat-poly(glycerol monomethacrylate)_y-poly(benzyl methacrylate)₃₀₀ [(**P_x-stat-G_y**)-**B₃₀₀**] nanoparticles

The synthesis of poly(2-(phosphonooxy)ethyl methacrylate)_x-stat-poly(glycerol monomethacrylate)_y-poly(benzyl methacrylate)₃₀₀ (**P₃₂-stat-G₁₃**)-**B₃₀₀**) diblock copolymer nanoparticles was conducted as follows. (**P₃₂-stat-G₁₃**) macro-CTA (130 mg, 15.2 μmol), ACVA (0.85 mg, 3.04 μmol , macro-CTA/ACVA molar ratio = 5.0), and methanol (3.30 g) were added to a 14 mL vial equipped with a magnetic stir bar and sealed with a rubber septum. Benzyl methacrylate (803 mg, 4.56 mmol) was added and the vial was placed in an ice bath. The stirred methanolic solution was degassed with N_2 for 30 min and the vial was then transferred to a preheated oil bath set at 70 °C. After 24 h, the polymerization was quenched by exposing the contents of the flask to air while cooling to ambient temperature. ^1H NMR studies indicated more than 99 % conversion. The resulting copolymer

nanoparticles were centrifuged (11,000 rpm for 30 min) after being diluted to 1.0 wt% using deionized water. The aqueous supernatant was carefully decanted and the sedimented nanoparticles were redispersed in deionized water. This centrifugation-redispersion cycle was repeated five times.

1.8. Precipitation of calcium carbonate crystals in the presence of nanoparticles

An aqueous solution (50.0 mL) containing CaCl_2 (1.0 mM) and various nanoparticles (0.1% w/w) was placed in a dessicator. CaCO_3 crystals were precipitated onto a glass slide (pre-cleaned using 'piranha' solution) placed at the base of this aqueous solution by exposure to ammonium carbonate vapor^[1] (2-3 g ammonium carbonate, placed at the bottom of the dessicator) for 24 h at 20 °C. Then the glass slide was removed from the solution and washed three times with deionized water, followed by three rinses with ethanol. Each occlusion experiment was repeated at least twice and consistent results were obtained in each case. The crystals at the bottom of each glass beaker (in addition to those deposited onto the glass slide) were carefully removed with the aid of a spatula and oven-dried for four days at 110 °C prior to TGA analysis.

2. Characterization

2.1. ^1H NMR spectroscopy

All ^1H NMR spectra were recorded using a Bruker Avance 400 spectrometer operating at 400 MHz using either D_2O , CD_3OD or $\text{d}_6\text{-DMSO}$ as the solvent.

2.2. Gel permeation chromatography (GPC)

The DMF GPC instrument set-up comprised two Polymer Laboratories PL gel 5 μm Mixed C columns and one PL polar gel 5 μm guard column connected in series to a Varian 390-LC multi-detector suite (only the refractive index detector was used) and a Varian 290-LC pump injection module operating at 60 °C. The GPC eluent was HPLC-grade DMF containing 10 mM LiBr and was filtered prior to use. The flow rate was 1.0 mL min^{-1} and DMSO was used as a flow-rate marker. Calibration was conducted using a series of ten near-monodisperse poly(methyl methacrylate) standards ($M_n = 6.25 \times 10^2 - 6.18 \times 10^5 \text{ g mol}^{-1}$, $K = 2.094 \times 10^{-3}$, $\alpha = 0.642$). Chromatograms were analyzed using Varian Cirrus GPC software.

Aqueous GPC analysis was performed using an Agilent Technologies Infinity 1260 set-up comprising two 8 μm PL Aquagel-OH 30 columns running at 30 °C, a UV detector (set at 301 nm), and a refractive index detector. The GPC eluent was an aqueous buffer comprising 200 mM NaNO_3 and 10 mM NaH_2PO_4 at pH 9 containing 30 vol% methanol co-solvent at a flow rate of 1.0 mL min^{-1} . Calibration was achieved using a series of near-monodisperse poly(ethylene oxide) standards ranging from 4.1×10^3 to $6.92 \times 10^5 \text{ g mol}^{-1}$.

2.3. Dynamic light scattering (DLS)

DLS measurements were conducted at 25 °C using a Malvern Zetasizer NanoZS instrument by detecting back-scattered light at 173°. Aqueous dispersions were diluted to 0.1% w/w using deionized water in the presence of 1.0 mM Ca^{2+} ions. The Stokes-Einstein equation was used to calculate the z-average particle diameter in each case. Aqueous electrophoresis measurements were conducted in the presence of varying CaCl_2 concentration (0-3.0 mM) using the same Zetasizer NanoZS instrument equipped with disposable folded capillary cells (DTS1070) supplied by Malvern.

2.4. Transmission electron microscopy (TEM)

TEM images were obtained using palladium-copper grids (Agar Scientific, UK). These grids were coated with a thin carbon film and then treated with a plasma glow discharge for approximately 30 seconds to create a hydrophilic surface prior to addition of the dilute sample dispersion (5 μ L, 0.1 % w/v). Excess solvent was removed via blotting and each grid was stained with uranyl formate for 30 seconds. Excess stain was removed via blotting followed by careful drying under vacuum. Imaging was performed using a FEI Tecnai G2 Spirit instrument operating at 80 kV.

2.5. Scanning electron microscopy (SEM)

Individual calcite crystals were fractured by placing a clean glass slide on top of the glass slide supporting the crystals, pressing down with light hand pressure and twisting one slide relative to the other. The resulting randomly-fractured calcite crystals were gold-coated (15 mA, 30 seconds) and then examined by scanning electron microscopy (FEI Inspect F instrument). A relatively low accelerating voltage (5 kV) was applied in order to prevent sample charging.

2.6. Other measurements

Optical microscopy images were recorded using a Motic DMBA300 digital biological microscope equipped with a built-in camera and analyzed using Motic Images Plus 2.0 ML software. Raman spectra were recorded using a Renishaw 2000 Raman microscope equipped with a 785 nm diode laser. Thermogravimetric analyses (TGA) were conducted using a Perkin-Elmer Pyris 1 TGA instrument by heating dried calcite crystals from 30 °C to 900 °C in air at a heating rate of 10 °C per min. Each sample was ground and dried at 110 °C for one week prior to TGA studies. The calculation method for the extent of nanoparticle occlusion based on TGA data is similar to that described in our earlier report.^[2]

3. Supplementary Tables

Table S1. Summary of mean diameter, zeta potential and density for a series of six sterically-stabilized diblock copolymer nanoparticles of varying anionic phosphate content.

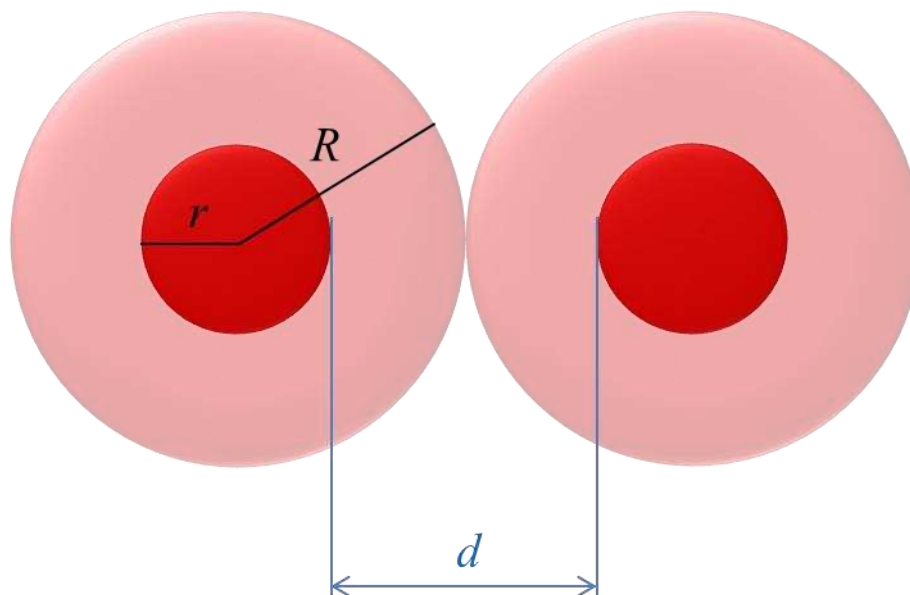
Copolymer ID	SEM diameter (nm)	DLS diameter (nm)	Zeta potential (mV)	DLS diameter in 1 mM Ca ²⁺ (nm)	Zeta potential in 1 mM Ca ²⁺ (mV)	Particle density (g cm ⁻³)
G ₅₁ -B ₃₀₀	74 ± 10	89 (0.08)	-7 ± 2	83 (0.09)	-5 ± 2	1.213
(P ₉ -stat-G ₃₇)-B ₃₀₀	122 ± 20	140 (0.04)	-43 ± 6	135 (0.05)	-24 ± 7	1.215
(P ₂₁ -stat-G ₂₅)-B ₃₀₀	106 ± 16	122 (0.01)	-52 ± 6	114 (0.02)	-21 ± 6	1.218
(P ₃₂ -stat-G ₁₃)-B ₃₀₀	100 ± 18	130 (0.02)	-58 ± 7	116 (0.02)	-20 ± 7	1.227
(P ₄₅ -stat-G ₇)-B ₃₀₀	104 ± 17	129 (0.01)	-61 ± 6	114 (0.01)	-18 ± 7	1.234
P ₅₁ -B ₃₀₀	118 ± 20	139 (0.01)	-62 ± 6	123 (0.02)	-18 ± 8	1.250

Table S2. Summary of the amounts of each comonomer and RAFT agent used for the synthesis of the various macro-CTAs. The [RAFT agent]/[initiator] molar ratio was 5.0 in each case.

Macro-CTA	RAFT agent (CPDB)		P monomer				G monomer			
	Mass (g)	Mole (mmol)	Mass (g)	Mole (mmol)	Target DP	Actual DP	Mass (g)	Mole (mmol)	Target DP	Actual DP
G ₅₁	0.460	2.0	-	-	-	-	20.0	125.0	60	51
P ₉ -stat-G ₃₇	0.169	0.76	0.8	3.81	5	9	5.49	34.3	45	37
P ₂₁ -stat-G ₂₅	0.158	0.71	1.5	7.14	10	21	4.57	28.6	40	25
P ₃₂ -stat-G ₁₃	0.211	0.95	3.0	14.3	15	32	2.29	14.3	15	13
P ₄₅ -stat-G ₇	0.200	0.91	4.0	19.0	21	45	1.31	8.16	9	7
P ₅₁	0.234	1.06	6.0	28.6	27	51	-	-	-	-

4. Calculation of the average inter-particle distance (d)

The volume fraction (p) of the occluded nanoparticles within the calcite crystal can be calculated from the mass loading indicated by TGA. The diblock copolymer nanoparticles prepared in this study are assumed to be perfectly monodisperse in order to calculate the average inter-particle distance (d).



Scheme S1. A 2D schematic cartoon showing the inter-particle distance (d), where r represents the nanoparticle core radius and R presents the radius of the virtual nanoparticle (i.e. the nanoparticle core plus a virtual shell) [N.B. This virtual shell is NOT the steric stabilizer layer but is instead the effective shell corresponding to randomly close-packed spheres].

Assuming that the nanoparticles have a virtual shell, the average inter-particle distance can be obtained by: $d = 2(R - r)$

The volume of a single nanoparticle core:

$$v = \frac{4}{3}\pi r^3 \dots \dots \dots (1)$$

The volume of a single virtual nanoparticle:

$$v' = \frac{4}{3}\pi R^3 \dots \dots \dots (2)$$

Thus the total volume of the nanoparticle cores within the crystal can be obtained by:

$$V_t = v \times N = \frac{4}{3}\pi r^3 \times N \dots \dots \dots (3)$$

Where v_t and N are the total volume and the number of occluded nanoparticles within the crystal, respectively.

The total volume of the virtual nanoparticles can be calculated using:

$$V'_t = v' \times N = \frac{4}{3}\pi R^3 \times N \dots \dots \dots (4)$$

Where V'_t and N are the total volume and the number of the occluded virtual nanoparticles within the crystal, respectively.

$$p = \frac{D \times V_t}{V'_t} \dots \dots \dots (5)$$

Where p is the volume fraction of occluded nanoparticles and D is the nanoparticle packing efficiency, respectively.

Thus,

$$d = 2(R - r) = 2r \left(\sqrt[3]{\frac{D}{p}} - 1 \right) \dots \dots \dots (6)$$

Theoretically, the packing efficiency for either hexagonally-packed or face-centred cubic-packed uniform nanoparticles is ≈ 0.74 . However, the distribution of the occluded nanoparticles within the calcite host crystals appears to be random, in which case their packing efficiency should be ≈ 0.64 .^[3]

5. Supplementary Figures

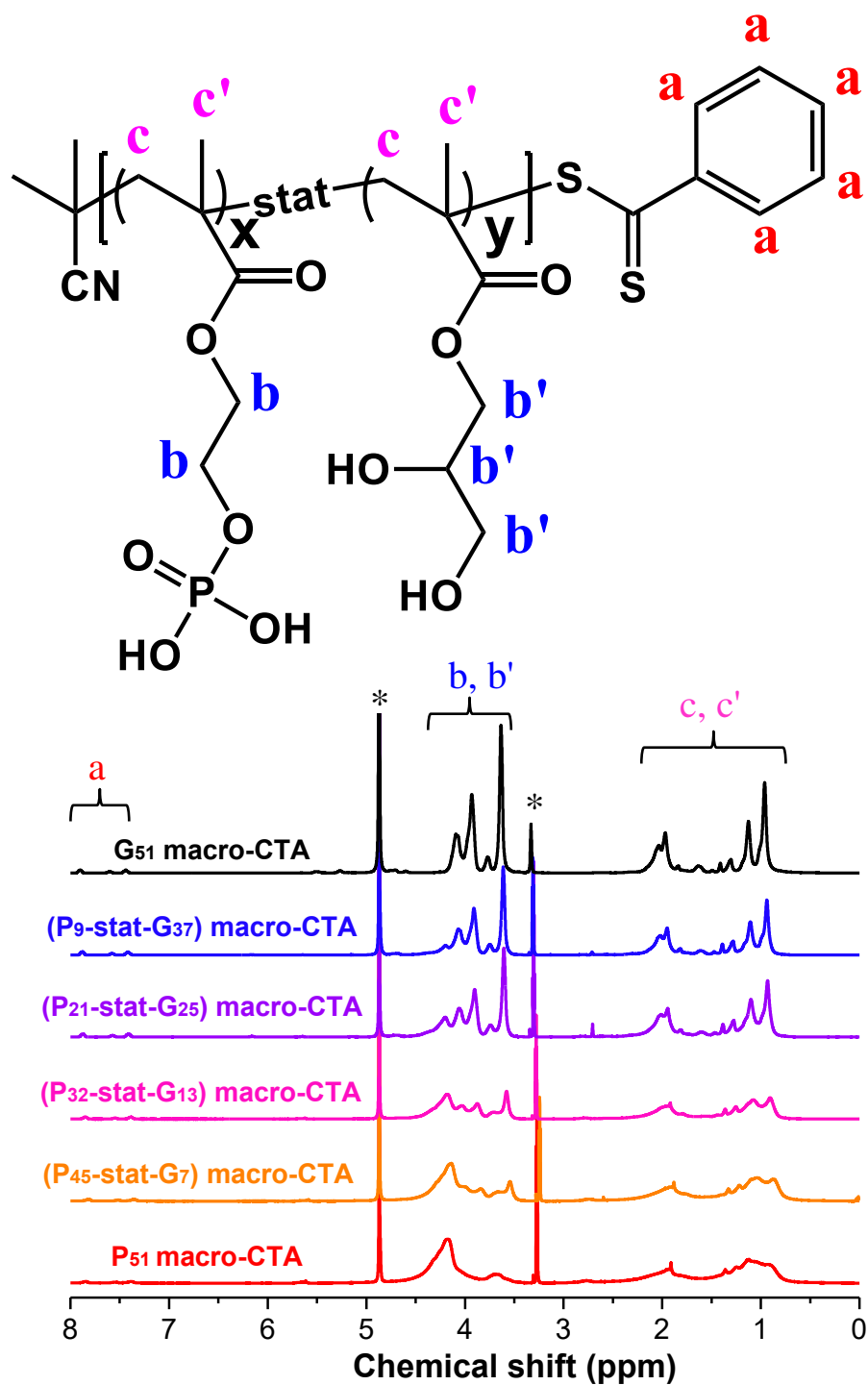


Figure S1. ¹H NMR spectra (CD₃OD) recorded for various steric stabilizer macro-CTAs.

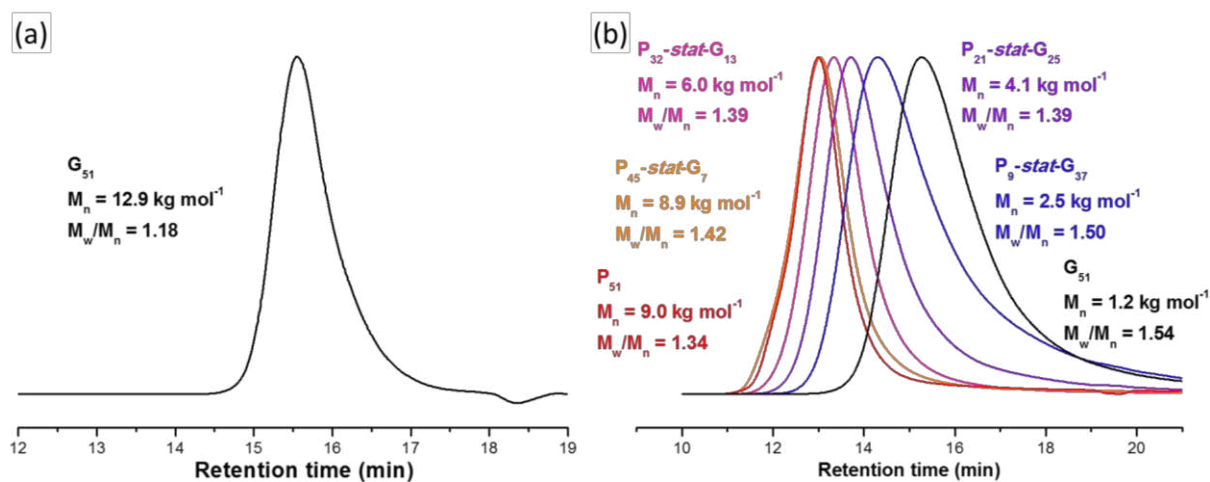


Figure S2. (a) DMF GPC curve recorded for G₅₁ macro-CTA; (b) Six aqueous GPC curves recorded for various macro-CTAs. GPC analysis of the G₅₁ macro-CTA using DMF eluent yielded an M_n of 12.9 kg mol⁻¹ and an M_w/M_n of 1.18, respectively. However, the apparent M_w/M_n of this macro-CTA increased significantly ($M_w/M_n = 1.54$) when analyzed by aqueous GPC. The precise reason for the latter artefact is not fully understood, but there is a striking correlation between the G content of these (co)polymers and the width of the corresponding molecular weight distribution. It is emphasized that each macro-CTA exhibits a unimodal curve, suggesting that these (co)polymerizations proceed under good RAFT control.

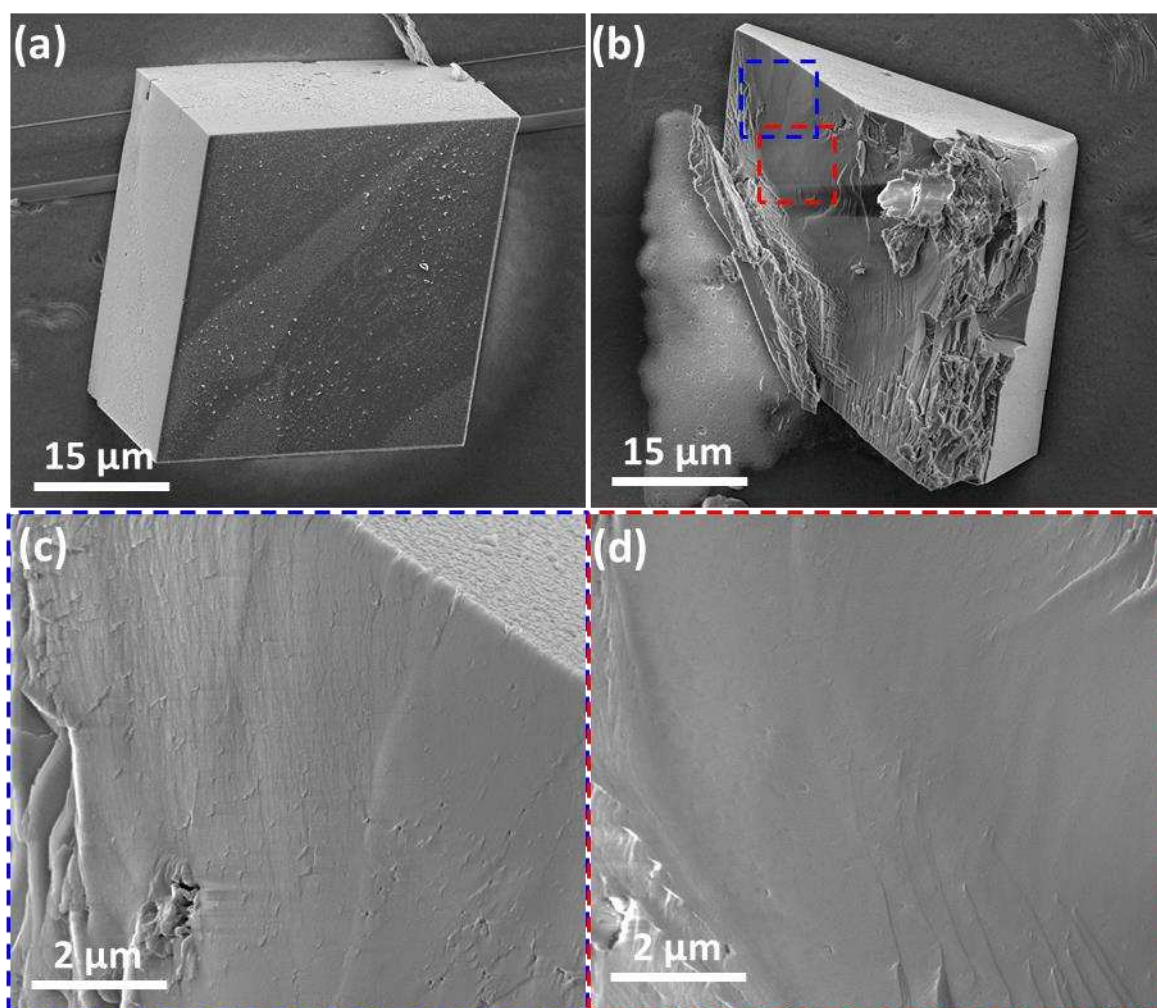


Figure S3. SEM images of CaCO₃ crystals precipitated in the absence of G₅₁-B₃₀₀ diblock copolymer nanoparticles: (a) low-magnification image showing a single intact CaCO₃ crystal; (b) internal structure of a randomly-fractured CaCO₃ crystal; (c) and (d) higher magnification images showing the areas indicated in (b).

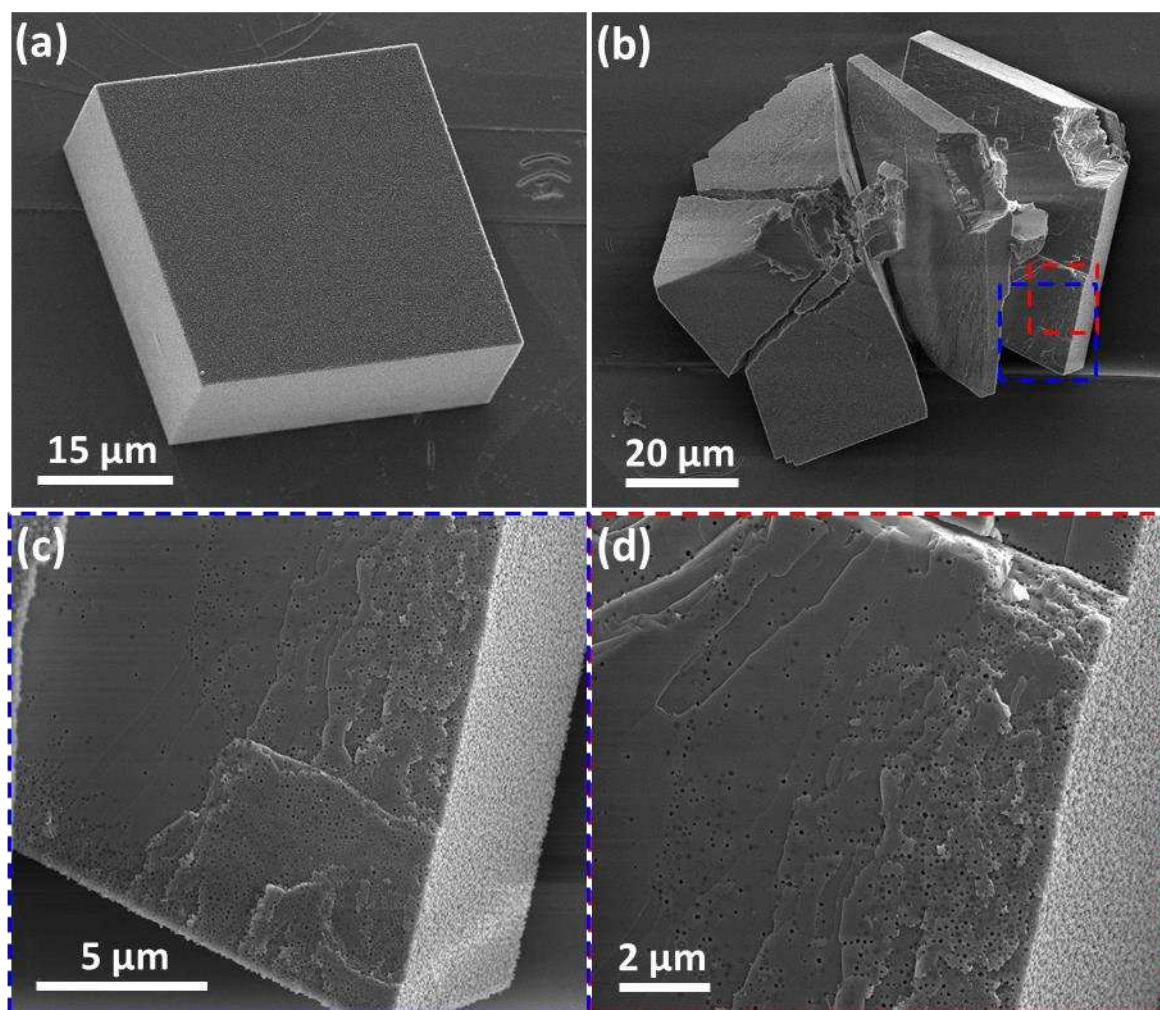


Figure S4. CaCO₃ crystals prepared in the presence of 0.1% w/w (P₉-stat-G₃₇)-B₃₀₀ nanoparticles: (a) low-magnification image showing a single intact CaCO₃ crystal; (b) internal structure of a randomly-fractured CaCO₃ crystal; (c) and (d) higher magnification images showing the areas indicated in (b).

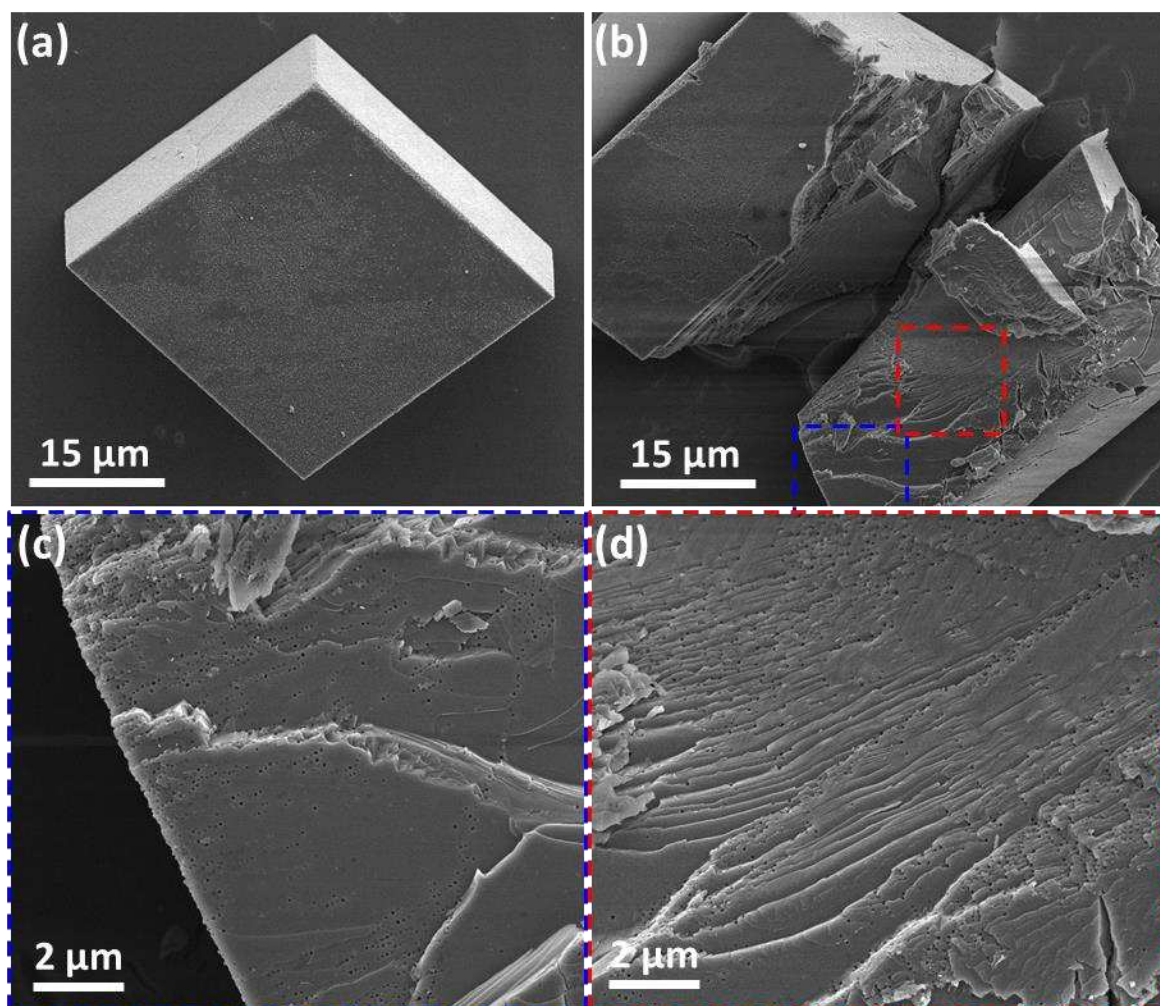


Figure S5. CaCO₃ crystals prepared in the presence of 0.1% w/w (P_{21-stat-G₂₅})-B₃₀₀ nanoparticles: (a) low-magnification image showing a single intact CaCO₃ crystal; (b) internal structure of a randomly-fractured CaCO₃ crystal; (c) and (d) higher magnification images showing the areas indicated in (b).

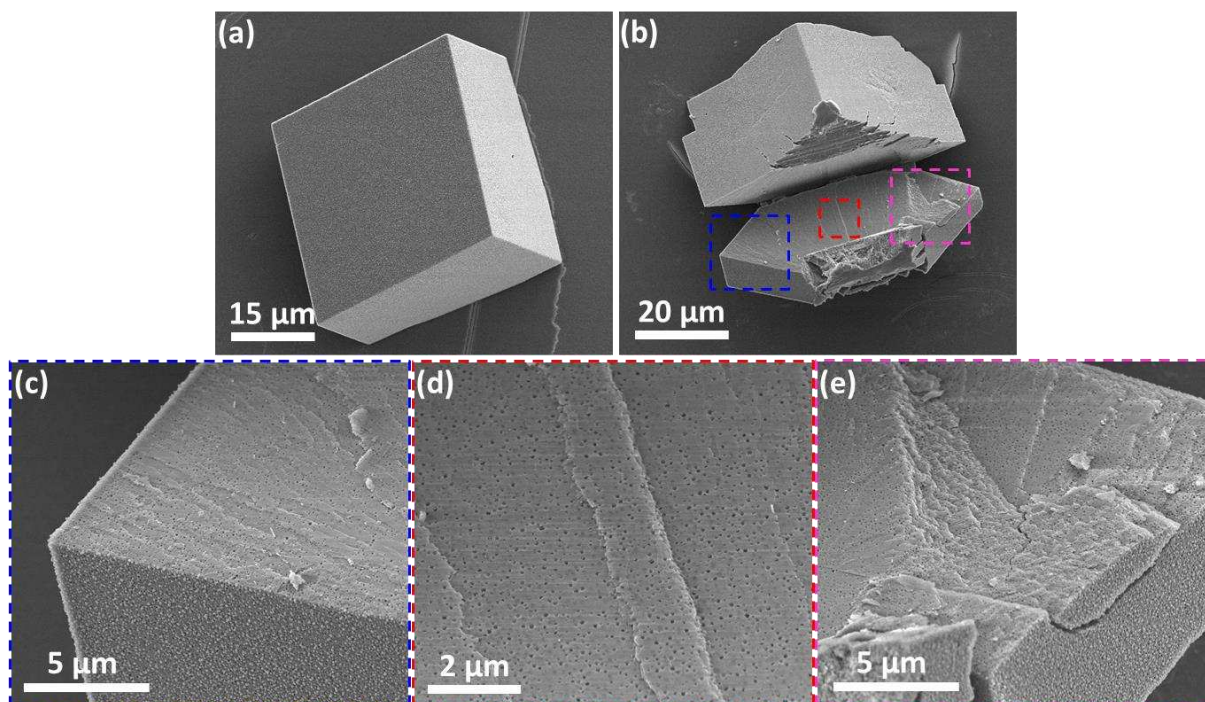


Figure S6. CaCO_3 crystals prepared in the presence of 0.1% w/w ($\text{P}_{32}\text{-stat-G}_{13}$)- B_{300} nanoparticles: (a) low-magnification image showing a single intact CaCO_3 crystal; (b) internal structure of a randomly-fractured CaCO_3 crystal; (c) ~ (e) higher magnification images showing the areas indicated in (b).

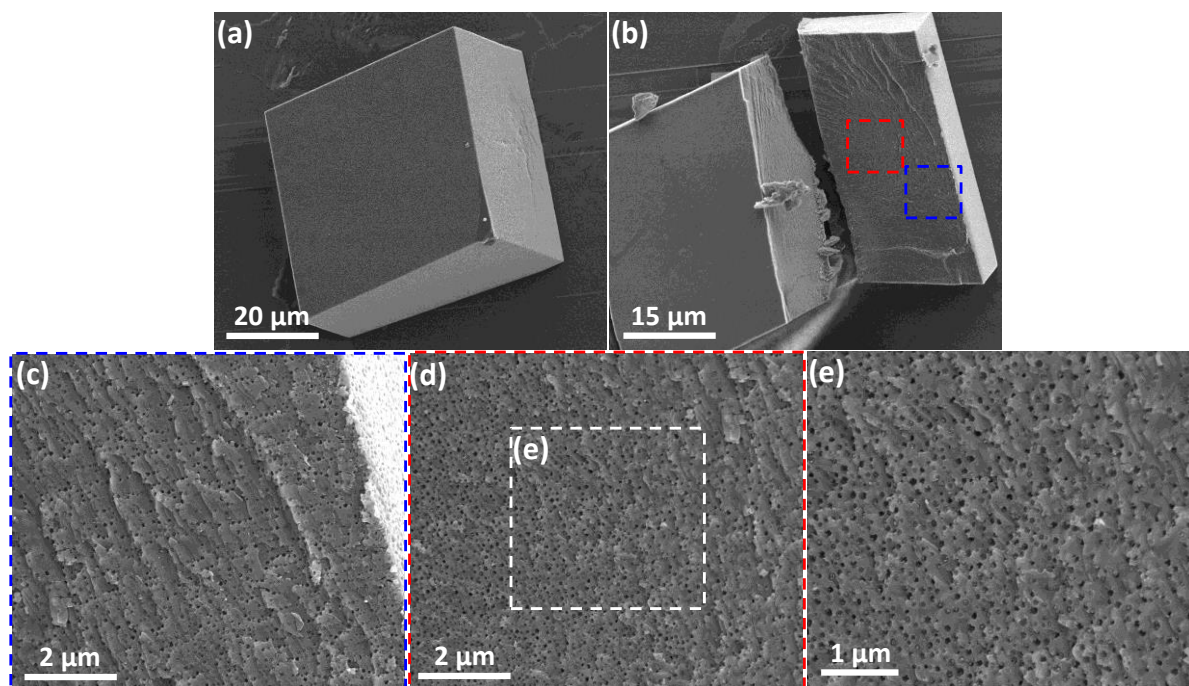


Figure S7. CaCO₃ crystals prepared in the presence of 0.1% w/w (P₄₅-stat-G₇)-B₃₀₀ nanoparticles: (a) low-magnification image showing a single intact CaCO₃ crystal; (b) internal structure of a randomly-fractured CaCO₃ crystal; (c) and (d) higher magnification images showing the areas indicated in (b).

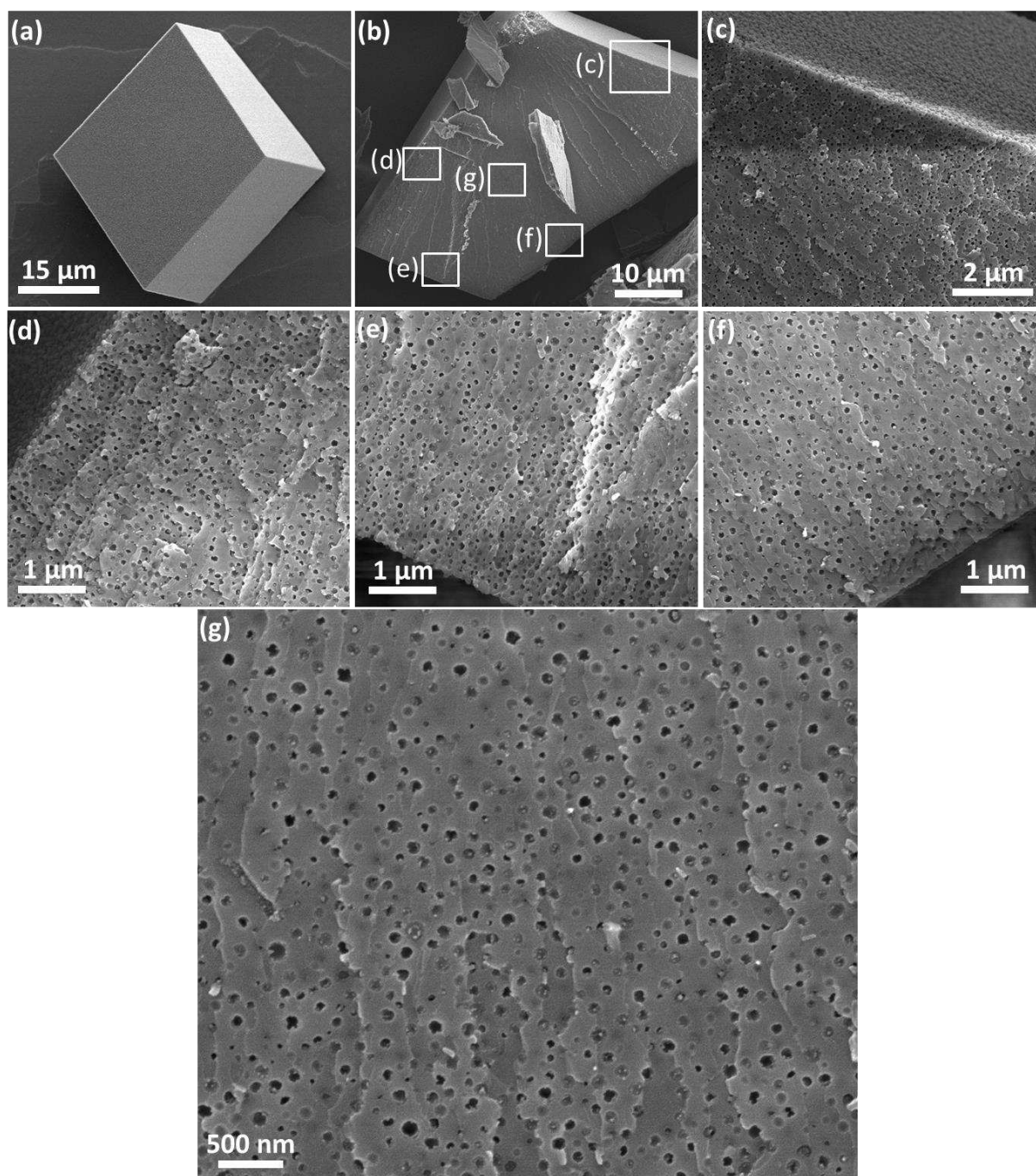


Figure S8. CaCO₃ crystals prepared in the presence of 0.1% w/w P₅₁-B₃₀₀ nanoparticles: (a) low-magnification image showing a single intact CaCO₃ crystal; (b) internal structure of a randomly-fractured CaCO₃ crystal; (c) ~ (g) higher magnification images showing the areas indicated in (b).

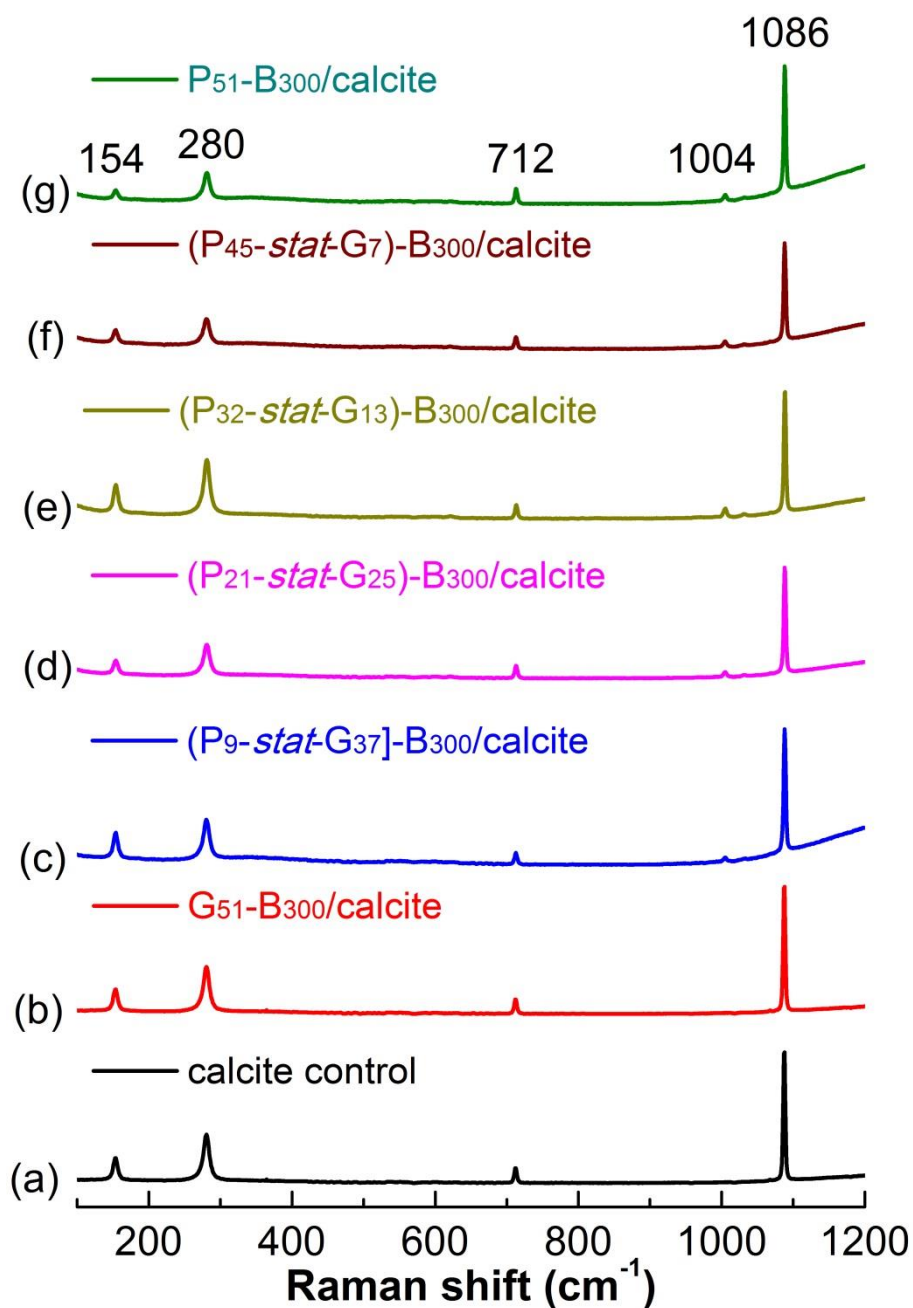


Figure S9. Raman spectra recorded for (a) pure calcite (control), and CaCO_3 samples prepared in the presence of six different (co)polymer nanoparticles: (b) $\text{G}_{51}\text{-B}_{300}$; (c) $(\text{P}_9\text{-stat-G}_{37})\text{-B}_{300}$; (d) $(\text{P}_{21}\text{-stat-G}_{25})\text{-B}_{300}$; (e) $(\text{P}_{32}\text{-stat-G}_{13})\text{-B}_{300}$; (f) $(\text{P}_{45}\text{-stat-G}_7)\text{-B}_{300}$; (g) $\text{P}_{51}\text{-B}_{300}$.

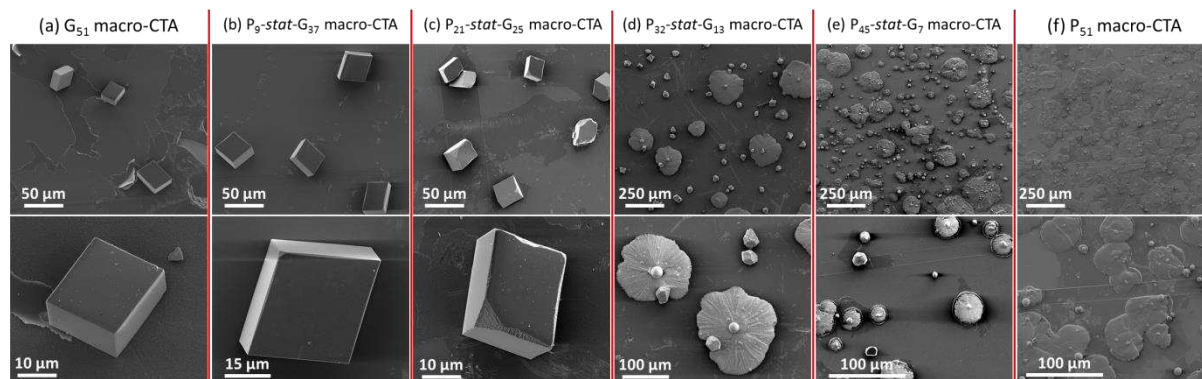


Figure S10. SEM images recorded for CaCO₃ prepared in the presence of various steric stabilizer macro-CTAs: (a) G₅₁; (b) (P₉-stat-G₃₇); (c) (P₂₁-stat-G₂₅); (d) (P₃₂-stat-G₁₃); (e) (P₄₅-stat-G₇); (f) P₅₁.

5. References

- [1] a) L. Addadi, J. Moradian, E. Shay, N. Maroudas, S. Weiner, *Proc. Natl. Acad. Sci.* **1987**, *84*, 2732-2736; b) J. Aizenberg, A. J. Black, G. M. Whitesides, *Nature* **1999**, *398*, 495.
- [2] Y. Ning, L. A. Fielding, L. P. D. Ratcliffe, Y.-W. Wang, F. C. Meldrum, S. P. Armes, *J. Am. Chem. Soc.* **2016**, *138*, 11734.
- [3] G. D. Scott, D. M. Kilgour, *J. Phys. D: Appl. Phys.* **1969**, *2*, 863.